



# Study on Quantitative Characterization of Morphological Characteristics and High Temperature Performance Evaluation of Coarse Aggregate Based on Computer Vision

Zhanliang Liu<sup>1,2</sup>, Chen Zhang<sup>1,3\*</sup>, Linlong Shao<sup>1</sup> and Jiangfeng Wang<sup>1</sup>

<sup>1</sup>Key Laboratory for Special Area Highway Engineering of Ministry of Education, Chang'an University, Xi'an, China, <sup>2</sup>Department of Railway Engineering, Shijiazhuang Institute of Railway Technology, Shijiazhuang, China, <sup>3</sup>School of Energy and Architecture, Xi'an Aeronautical University, Xi'an, China

## OPEN ACCESS

### Edited by:

Hui Yao,  
Beijing University of Technology,  
China

### Reviewed by:

Jiaying Hu,  
Southeast University, China  
Yunchao Tang,  
Zhongkai University of Agriculture and  
Engineering, China

### \*Correspondence:

Chen Zhang  
865916600@qq.com

### Specialty section:

This article was submitted to  
Structural Materials,  
a section of the journal  
Frontiers in Materials

**Received:** 16 September 2020

**Accepted:** 30 November 2020

**Published:** 02 February 2021

### Citation:

Liu Z, Zhang C, Shao L and Wang J  
(2021) Study on Quantitative  
Characterization of Morphological  
Characteristics and High Temperature  
Performance Evaluation of Coarse  
Aggregate Based on Computer Vision.  
*Front. Mater.* 7:607105.  
doi: 10.3389/fmats.2020.607105

The morphological characteristics of aggregate include outline shape, angularity, and surface texture, which determine the mutual extrusion and friction between aggregates, and significantly affect the performance of asphalt pavement. At present, the research on the morphological characteristics of coarse aggregate is mainly focused on indoor visual identification technology (AIMS, XCT, etc.), in which the applicability of the proposed aggregate shape characterization index is weak, and these instruments could not serve the practical engineering well. In this article, the Coarse Aggregate Morphological Identification System (CAMIS) is developed based on computer vision technology, and the system can recognize the shape features of aggregates above 2.36 mm particle size and carry out uninterrupted feeding and removal based on the mechanical arm system, which can realize large sample detection. Based on CAMIS aggregate identification system and laboratory tests (rutting test, dynamic modulus test, and penetration shear test), the shape identification and performance test of aggregate samples from construction site are carried out, and an aggregate performance evaluation index, CEI, suitable for high-temperature areas is proposed in combination with the improved response surface method. The processing parameters of vertical shaft impact aggregate crusher are optimized based on the CEI index, and the recommended processing parameters are verified by laboratory tests. The results show that the morphological characteristics of coarse aggregate affect the high temperature performance in order angularity, needle flake, axial coefficient, and convexity. The combination of processing parameters of vertical axis impact crusher is recommended to be of 45 m/s rotational speed, 3 t/h feed quantity, and 30% air intake. Verified by laboratory tests, the aggregate identification system CAMIS developed in this article and the proposed aggregate performance evaluation index, CEI, are highly reliable.

**Keywords:** asphalt pavement, coarse aggregate, computer vision, technology, mesomorphology, quantitative characterization, performance evaluation

## INTRODUCTION

The morphological characteristics of aggregate include outline shape, angularity, and surface texture, which are closely related to the formation of asphalt mixture spatial skeleton and the interaction between asphalt and aggregate, significantly affecting the road performance of asphalt mixture (Li et al., 2019). The shape, angularity, and surface texture of coarse aggregate determine the intercalation and friction between aggregates and make a certain contribution to the formation of good mechanical properties and structural strength of asphalt mixture. It is a key factor for asphalt pavement to overcome permanent deformation (Zhang et al., 2012). Many scholars have done in-depth research on the acquisition and characterization of morphological characteristics of coarse aggregate. Al-Rousan et al. (2007) revealed that the influence of coarse aggregates angularity and shape on the performance of asphalt mixture is significant, but the existing research techniques cannot distinguish the effect of angularity and shapes. Arasan et al. (2011) used the DIP technique to study the morphological characteristics of the aggregate and proposed some new evaluation indexes such as elongation and roundness. Rezaei and Masad (2013) quantitatively characterize the relationship between aggregate morphology and pavement skid resistance using the data of laboratory test and field investigation. In recent years, some scholars have used X-ray tomography (XCT) to obtain internal continuous tomographic images to reflect the three-dimensional spatial structure information of materials. The digital image obtained based on XCT technology can show the three-dimensional structural and geometric features of coarse aggregate more accurately and truly. Wang et al. (2016) used a modified Los Angeles Abrasion Test (LAAT) to change the shape of the aggregate and studied the correlation between aggregate shape parameters and high temperature performance of asphalt mixture. Ding et al. (2017) obtained the realistic shape of granular aggregates and made the statistical analysis to quantify the morphological differences. Ghuzlan et al. (2019) proposed the flatness index and roundness index as morphological evaluating indexes of coarse aggregate based on the image identification and image processing techniques. Kuang et al. (2019) proved that the average angular coefficient of coarse aggregate is also correlated with the high temperature stability, water stability, and low temperature performance of asphalt mixture. Singh et al. (2013) compared the morphological characteristic parameters (angularity, texture, and flatness) of aggregates with different lithologies (granite, rhyolite, and limestone) and found that the morphological characteristic parameters of coarse aggregate of different lithologies are different. Liu et al. (2016) optimized the Fourier transform interferometry (FTI) system and used the sphericity, flatness, elongation, angularity, and surface texture to identify the morphological characteristics of coarse aggregate. Kwon et al. (2017) studied the relationship between the aggregate morphology and the permanent deformation capacity of asphalt mixture and analyzed the key factors affecting the permanent deformation of the asphalt mixture. Wang et al. (2019a) proposed the sphericity, flatness, elongation, angularity, and surface texture

index to describe the morphological characteristics of coarse aggregate based on the AIMS experiment instruments. Thus, the research on the morphological characteristics of coarse aggregate is mainly focused on indoor visual identification technology (AIMS, XCT, etc.). The proposed aggregate shape characterization index lacks pertinence, and the testing equipment cannot effectively provide services for asphalt mixture site construction control because of economy and portability (Plati et al., 2016).

Through the limited experimental design of the set of sample points in the specified design space, the response surface method fits the global approximation of the output variable (system response) to replace the real response surface (Mohamed et al., 2016). However, for the morphological characteristics of coarse aggregate, the optimal solution corresponding to different evaluation indexes is different. Therefore, the traditional response surface design method needs to be improved. The improved method is to use gray correlation analysis according to different high temperature evaluation indexes. The comprehensive evaluation method of gray correlation degree can give an evaluation value to each evaluation index of the evaluation object according to the given conditions, so as to comprehensively judge the evaluation object under the interaction of multiple factors (Luo et al., 2016).

Machine vision is a modern comprehensive measurement technology that has been active in recent years, covering a wide range of fields, including computer vision, digital image processing, digital signal analysis, pattern recognition, artificial intelligence, and other technologies. In simple terms, it is to use a camera instead of the human eye to identify and judge the target object to be detected. First, the target image is acquired through the visual sensor, and then the image is transmitted to the host computer for a series of analyses such as digital image processing, and finally according to the pixel point distribution or image color, brightness and other information are used to complete the detection of target size, shape, and color. Chen et al. (2019) discussed the causes of global calibration errors in detail and built a four-camera vision system to obtain the visual information of targets including static objects and a dynamic concrete-filled steel tubular (CFST) specimen. Tang et al. (2019) presented a dynamic real-time detection method for surface deformation and full field strain in recycled aggregate concrete-filled steel tubular columns (RACSTCs). Majidifard et al. (2020) developed a U-net based model to quantify the severity of the pavement distresses and a hybrid model by integrating the YOLO and U-net models to classify the pavement distresses and quantify their severity simultaneously. Liu et al. (2019) adopted U-Net to detect the concrete cracks, and U-Net is found to be more elegant than DCNN with more robustness, more effectiveness, and more accurate detection. Wang et al. (2019b) used neural network technology to assist the robot patrol in an unknown work environment and to use faster R-CNN methods to find scattered nails and screws in real time, so that the robot can automatically recycle nails and screws.

Based on this, an expressway in Guangdong province is selected as a practical case, and a self-developed fast recognition system for the morphological characteristics of

**TABLE 1** | Basic performance test of aggregate.

Technical index	Test value	Specification requirements	Testing method
Crushing value (%)	12.3	≤26	T0316
Los Angeles wear loss (%)	15.4	≤28	T0317
Polishing value (%)	45	≥42	T0321
Water absorption rate (%)	0.60	≤2.0	T0304
Apparent density (g/cm <sup>3</sup> )	2.95	≥2.6	T0304

**TABLE 2** | The technical performance indexes of SBS modified asphalt.

Index	Units	Technical standards	Test results	Test methods
Penetration (25°C, 5 s, 100 g)	0.1 mm	60 ~ 80	69.5	T 0604
Softening point	°C	≥70	70.4	T 0606
Ductility (5°C)	cm	≥35	35.8	T 0605
Difference value of softening point in 48 h	°C	≤2.5	0.25	T 0606

coarse aggregate is used to quickly identify the needle flake, axial coefficient, angularity, and convexity of the aggregate used in the field engineering. Based on the Gray Correlation Response Surface Design method (GCRSD), the coarse aggregate monomer index is associated with dynamic stability, dynamic modulus, maximum shear stress, and internal friction angle. The evaluation index of aggregate performance suitable for the study area is put forward, and the reasonable operation parameters of aggregate processing equipment are recommended to reveal the road performance of asphalt mixture from the point of view of aggregate shape characteristics, so as to realize the effective control of asphalt pavement construction quality.

## OBJECTIVE

In order to enhance the applicability of mesomorphological characterization index of road aggregate, this research puts forward an aggregate performance evaluation index, CEI, which is suitable for high-temperature areas based on CAMIS aggregate identification system and laboratory test combined with improved response surface method. Finally, the processing parameters of vertical shaft impact aggregate crusher are optimized based on CEI index.

## RAW MATERIALS

### Aggregate

The basalt aggregate used in this study comes from the construction site, and the technical index of the aggregate is tested, as shown in **Table 1** (JTG E42-2005, 2005).

### Asphalt

SBS modified asphalt was employed in this study, and the content of SBS modifier is 3%. The technical performance indexes of SBS modified asphalt are shown in **Table 2**.

According to the situation of pavement construction on site, SMA-16 is selected as the gradation in this article, the best dosage of asphalt is 5.2%, and the amount of fiber is 0.3%.

## RESEARCH METHOD

### Aggregate Identification System

Based on the previous research results, the morphological characteristics of coarse aggregate are characterized by edge and angularity parameters, needle-like content, axial coefficient, and convexity (Gao et al., 2018). The specific algorithm of each index is as follows.

#### (1) Angular Value

Angular value is the square of the ratio of the circumferential polygon perimeter  $P_c$  to the equivalent elliptical perimeter  $P_E$ , which can characterize the angular properties of the particles. The larger the value, the better the angular property of the particles, such as

$$A_p = \left( \frac{P_c}{P_E} \right)^2 \quad (1)$$

#### (2) Needle Flake Content

Through the image recognition technology, the maximum length  $L$ , the maximum width  $w$ , and the maximum thickness  $t$  of the maximum length surface are determined ( $t < w < L$ ). The particles with  $L/t \geq 3$  are screened out as needle-like particles. Because the density of the same aggregate is the same, the needle-like content is calculated directly by volume. The equivalent ellipsoid method is used to calculate the needle-like particle volume  $V_i$  and the total aggregate volume  $V$ , as shown in (2). Finally, the needle-like content is calculated, as shown in (3).

$$V_i = \frac{4}{3} \pi L \times w \times t \quad (2)$$

$$Q_e = \frac{m_i}{M} \times 100 = \frac{V_i}{V} \times 100 \quad (3)$$

### (3) Axial Coefficient

The axial coefficient characterizes the needle-like size of the particles, and the larger the axial coefficient is, the greater the needle-like property of the particles is. It reflects the macroscopic state and characteristics of aggregate particles, and the calculation formula is shown in

$$A = L/W \quad (4)$$

In the formula,  $L$  is the maximum length of the particle equivalent ellipse and  $W$  is the secondary axis width of the particle equivalent ellipse.

### (4) Convexity

The original intention of the design of the convexity index is to consider that the coarse aggregate rapid identification system can directly measure the actual area of a particle  $S_A$  and calculate its circumscribed polygon area  $S_C$ . The convexity is the square root of the ratio of these two quantities, as shown in

$$C_R = \sqrt{\frac{S_A}{S_C}} \quad (5)$$

Based on the Python Programming Language and the above algorithms, a Coarse Aggregate Morphological Identification System (CAMIS) is developed independently, as shown in **Figure 1**.

The principle of the system is to first binarize the original aggregate image, then reduce the noise of the aggregate image, then calculate the geometric parameters of each aggregate based on the OPENCV computer vision module, and finally calculate the needle-like content, axial coefficient, angular value, and convexity of the coarse aggregate. The system can identify the shape characteristics of aggregates above 2.36 mm particle size and carry out uninterrupted feeding and removal based on the mechanical arm system, which can achieve large sample detection and improve the accuracy of calculation results. The response time of single aggregate result is less than 1 s.

## Improved Response Surface Method

First of all, the response surface design uses the sequential method to observe and analyze the factors that affect the response variables one by one and then uses the Box-Behnken central combination design method to design the experiment with four factors and three levels, so as to establish the quadratic equation of the response surface and use the mathematical method to find the optimal solution. The weight distribution of several evaluation indexes is carried out to determine the evaluation index value of the morphological index of coarse aggregate to the high temperature performance of asphalt mixture (Shen et al.,

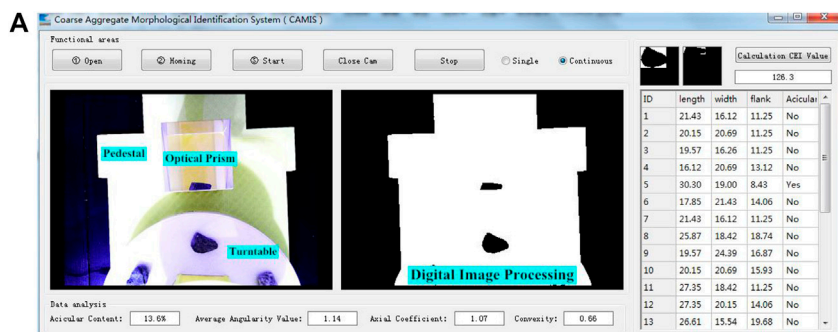
2014). In this study, the calculation processes of improved response surface method are as follows.

- (1) The angular value  $X_1$ , needle flake content  $X_2$ , axial coefficient  $X_3$ , and convexity  $X_4$  are selected as the four factors affecting the high temperature performance of asphalt mixture, and the evaluation indexes of high temperature performance of asphalt mixture are determined. The evaluation indexes of high temperature performance of asphalt mixture are dynamic stability, dynamic modulus, maximum shear stress, and internal friction angle. And the corresponding evaluation index value of high temperature performance of asphalt mixture is determined.
- (2) The aggregate of a stone factory in Guangdong Province is selected, and the local aggregate is scanned and tested by using the rapid recognition system of coarse aggregate morphological characteristics, and the ranges of angular value  $X_1$ , needle-like content  $X_2$ , axial coefficient  $X_3$ , and convexity  $X_4$  are determined.
- (3) Box-Behnken design (BBD) with four factors and three levels is used to carry on the response surface test design.
- (4) The gray correlation analysis is used to analyze the impact factor of four coarse aggregate morphological indexes on each response value, and the correlation degree between morphological index and each high temperature performance evaluation index is calculated. As a result, the proportion of each high temperature performance evaluation index in evaluating the high temperature performance of asphalt mixture can be calculated.
- (5) According to the proportion, the evaluation index values of each group of tests are calculated by comprehensively considering the dynamic stability, dynamic modulus, maximum shear stress, and internal friction angle, and the evaluation index value is taken as the response value for the establishment of the model.
- (6) The response surface test data were analyzed by quadratic multinomial regression fitting, analysis of variance, significance test, and response surface analysis with Design-Expert 8.0 software.
- (7) Finally, the model is constructed; that is, the functional relationship between each coarse aggregate shape index and evaluation index value is established.

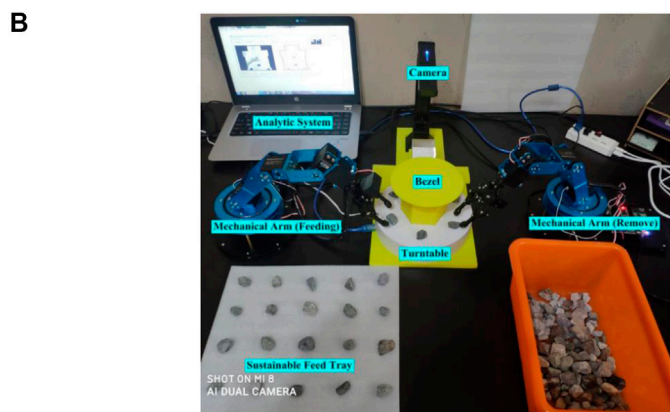
## RESULTS AND DISCUSSION

### High Temperature Performance Test Sampling and Morphological Testing of Aggregates

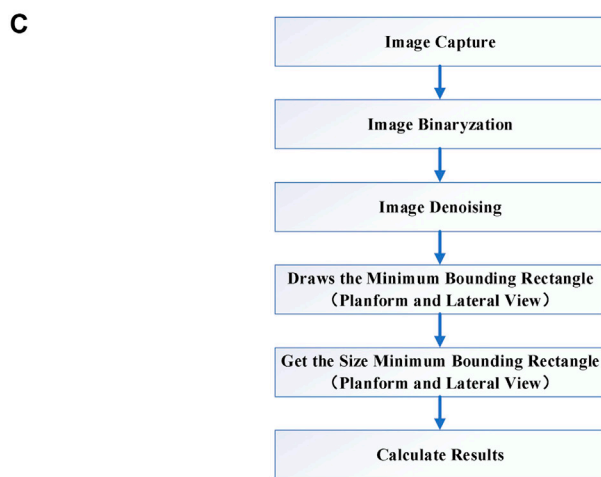
The basalt aggregates used in the field were sampled and equally divided into 29 parts, which were used in rutting test, dynamic modulus test, and penetration shear test, respectively. The self-developed aggregate shape recognition system (CAMIS) is used to test the aggregate shape, and the average value of the 29 groups of aggregate shape data is shown in **Table 3**.



Analysis Software



Hardware Equipment



Flowchart of CAMIS system

FIGURE 1 | Coarse aggregate morphological identification system. (A) Analysis software. (B) Hardware equipment. (C) Flowchart of CAMIS system.

### Rutting Test

The above 29 groups of aggregates with different morphological characteristics were used to form rutting specimens, and the automatic rut instrument was used to determine the dynamic stability of asphalt mixture. The size of the specimen is 300 × 300 × 50 mm, the total load applied is 780 N, the test wheel pressure is 0.7 ± 0.05 MPa, the loading rate is 42 times/min, and the test temperature is 60°C.

According to the “Standard Test Methods of Bitumen and Bituminous Mixtures for Highway Engineering (JTGE20-2011),” the test results of dynamic stability of asphalt mixture are shown in Figure 2.

### Dynamic Modulus Test

In all the asphalt pavement designs based on mechanical methods, the modulus of asphalt mixture is one of the most

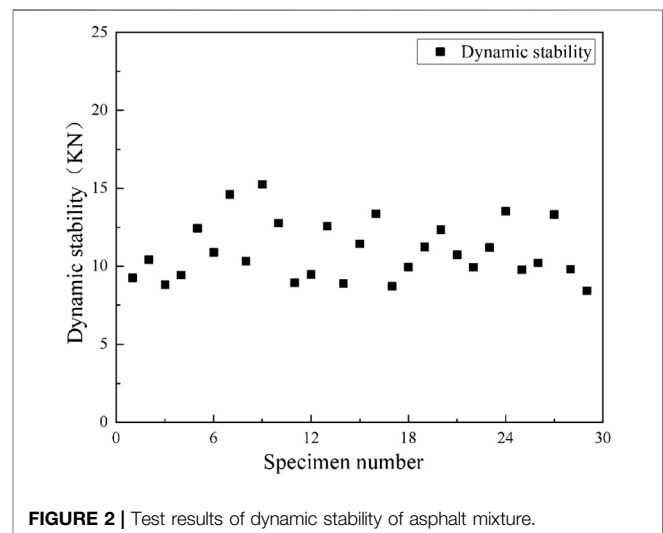
**TABLE 3** | Average value of sample aggregate shape data.

Group ID	Acicular content $X_1$	Average angularity value $X_2$	Axial coefficient $X_3$	Convexity $X_4$
	(Dimensionless)	(%)	(Dimensionless)	(Dimensionless)
1	1.15	16.20%	1.18	0.96
2	1.15	12.50%	1.18	0.46
3	1.15	14.35%	1.45	0.46
4	1.15	16.20%	1.18	0.46
5	1.10	14.35%	0.90	0.71
6	1.15	16.20%	1.45	0.71
7	1.15	14.35%	1.18	0.71
8	1.10	12.50%	1.18	0.71
9	1.15	14.35%	0.90	0.46
10	1.15	14.35%	1.18	0.71
11	1.15	14.35%	0.90	0.96
12	1.19	14.35%	1.18	0.96
13	1.15	12.50%	0.90	0.71
14	1.15	12.50%	1.18	0.96
15	1.15	14.35%	1.18	0.71
16	1.19	12.50%	1.18	0.71
17	1.15	16.20%	0.90	0.71
18	1.19	14.35%	1.45	0.71
19	1.19	14.35%	0.90	0.71
20	1.15	14.35%	1.18	0.71
21	1.15	12.50%	1.45	0.71
22	1.10	14.35%	1.18	0.46
23	1.10	16.20%	1.18	0.71
24	1.15	14.35%	1.45	0.96
25	1.15	14.35%	1.18	0.71
26	1.19	16.20%	1.18	0.71
27	1.19	14.35%	1.18	0.46
28	1.10	14.35%	1.45	0.71
29	1.10	14.35%	1.18	0.96

important parameters, and it is also the bridge between material performance and pavement structure. Therefore, the high temperature performance of asphalt mixture can be considered from the point of view of modulus (Lei et al., 2015). In this research, the dynamic modulus of asphalt mixture is measured by UTM-30, the cylindrical specimens with diameter of  $100 \pm 0.2$  mm and high  $150 \pm 0.2$  mm are formed by rotary compactor (SGC), and the asphalt mixture is molded with coarse aggregates with different morphological characteristics. There are 29 groups of specimens and there are three parallel specimens in each group, and the test results are taken as the average. Combined with the local climate and traffic conditions, the loading frequency is 0.5 hz and the experimental temperature is  $60^\circ\text{C}$ . The test results are shown in **Figure 3**.

### Penetration Shear Test

There is a good corresponding relationship between the penetration shear test index and the high temperature performance of asphalt mixture; the test parameters are easy to determine and have a good engineering application prospect (Tasdemir, 2009). Same as above, 29 groups of aggregate forming mixtures with different morphological characteristics are used, and the size of the specimen is  $100 \times 63.5$  mm pieces. There are 29 groups of specimens, each group has three parallel specimens,

**FIGURE 2** | Test results of dynamic stability of asphalt mixture.

and the test results are taken as the average. The loading rate is 1 mm hammer min, the size of the indenter is 28.5 mm, the test is carried out at  $60^\circ\text{C}$ , and finally the maximum shear stress and internal friction angle are obtained. The results are shown in **Figure 4**.

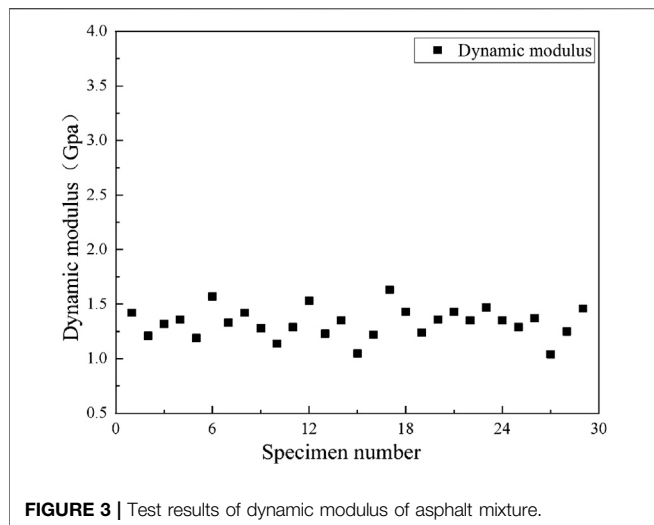


FIGURE 3 | Test results of dynamic modulus of asphalt mixture.

### Effect of Morphological Characteristics of Aggregate on High Temperature Performance of Mixture

Based on the aggregate shape data in Table 2, the response surface test factor level is established, as shown in Table 4.

The dynamic stability, dynamic modulus, maximum shear stress, and internal friction angle of asphalt mixture are used as control indexes to evaluate the high temperature stability of asphalt mixture. Four factors and three levels of test design are carried out by using Box-Behnken central combination design method, with a total of 29 groups of tests (Mourabet et al., 2012).

Combined with the test results in High Temperature Performance Test, the average value of each index is obtained by the method of gray correlation degree, in order to evaluate the influence of coarse aggregate shape index on the high temperature performance of mixture. The correlation degree analysis is shown in Table 5.

From the data in the Table 5, it can be seen that the influence degree of various morphological characteristics of coarse aggregate on high temperature evaluation index from high to low is angularity parameter > needle flake content > axial coefficient > convexity. Among them, the impact factor of angularity on the high temperature performance of asphalt mixture is the highest, while the influence of convexity is the least, which is consistent with the previous research results and the actual test results. Generally speaking, the coarse aggregate is rich in edges and corners, and when the surface texture is rougher, the mixture can form a good squeezing effect after compaction, which can increase the internal friction angle of the asphalt mixture and improve the strength of the asphalt mixture, and then improve the high temperature deformation resistance of asphalt mixture. The void age of asphalt mixture and the void age of mineral aggregate gradually increase with the increase of needle-like particle content of aggregate, while the asphalt saturation of gross bulk density decreases. The increase of

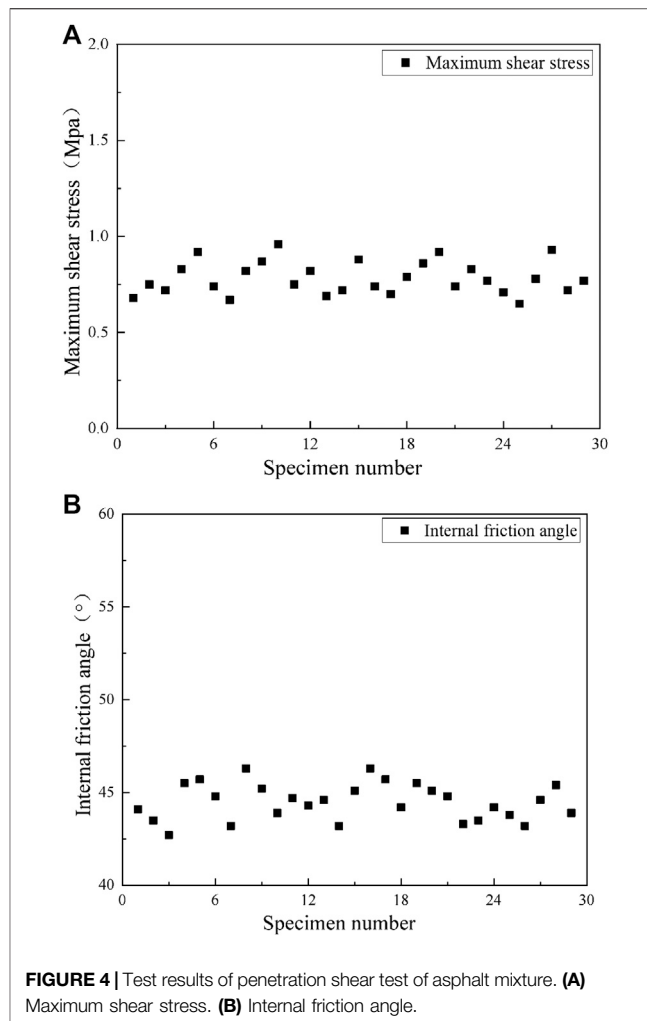


FIGURE 4 | Test results of penetration shear test of asphalt mixture. (A) Maximum shear stress. (B) Internal friction angle.

TABLE 4 | Response surface test factor level.

Factors	Level		
	-1	0	1
X <sub>1</sub> (angular value)	1.10	1.15	1.19
X <sub>2</sub> (needle flake content)	12.50	14.35	16.20
X <sub>3</sub> (axial coefficient)	0.90	1.18	1.45
X <sub>4</sub> (convexity)	0.46	0.71	0.96

Note: -1, 0, 1 represents the different value levels of the index.

needle-like content will reduce the high temperature stability of asphalt mixture to some extent.

### Construction of High Temperature Performance Evaluation Model of Aggregate Model Establishment

Based on the gray correlation analysis between the morphological eigenvalues of coarse aggregate and the high temperature

**TABLE 5** | Correlation between morphological characteristics and high temperature performance index.

Morphological index	Performance index			
	Dynamic stability	Dynamic modulus	Maximum shear stress	Internal friction angle
$X_1$ (angular value)	0.75	0.77	0.78	0.89
$X_2$ (needle flake content)	0.71	0.76	0.74	0.79
$X_3$ (axial coefficient)	0.70	0.68	0.67	0.71
$X_4$ (convexity)	0.68	0.62	0.62	0.68

**TABLE 6** | Response surface test design.

ID	$X_1$	$X_2$	$X_3$	$X_4$	Dynamic stability		Dynamic modulus		Maximum shear stress		Internal friction angle		CEI
					MV	CC	MV	CC	MV	CC	MV	CC	
					1	1.15	16.20	1.18	0.96	0.60	0.60	0.70	
2	1.15	12.50	1.18	0.46	0.79	0.79	0.79	0.69	0.75	0.75	43.5	0.70	123.87
3	1.15	14.35	1.45	0.46	0.62	0.62	0.71	0.71	0.63	0.63	42.7	0.61	118.86
4	1.15	16.20	1.18	0.46	0.67	0.67	0.73	0.73	0.72	0.72	45.5	0.62	126.69
5	1.10	14.35	0.90	0.71	0.67	0.67	0.70	0.70	0.55	0.55	45.7	0.43	133.37
6	1.15	16.20	1.45	0.71	0.83	0.83	0.69	0.69	0.69	0.69	44.8	0.55	128.87
7	1.15	14.35	1.18	0.71	0.53	0.53	0.95	1.00	0.66	0.66	43.2	0.65	132.67
8	1.10	12.50	1.18	0.71	0.89	0.89	0.88	0.69	0.52	0.78	46.3	0.72	130.61
9	1.15	14.35	0.90	0.46	0.42	0.42	0.85	0.67	0.57	0.57	45.2	0.66	138.65
10	1.15	14.35	1.18	0.71	0.70	0.70	0.86	0.62	0.41	0.56	43.9	0.53	130.03
11	1.15	14.35	0.90	0.96	0.66	0.66	0.77	0.67	0.43	0.69	44.7	0.69	123.49
12	1.19	14.35	1.18	0.96	0.65	0.65	0.89	0.61	0.41	0.80	44.3	0.78	124.71
13	1.15	12.50	0.90	0.71	0.63	0.63	0.83	0.73	0.48	0.78	44.6	0.76	130.97
14	1.15	12.50	1.18	0.96	0.55	0.65	0.83	0.73	0.46	0.70	43.2	0.65	120.21
15	1.15	14.35	1.18	0.71	0.78	0.90	0.86	0.52	0.42	0.70	45.1	0.70	129.35
16	1.19	12.50	1.18	0.71	0.62	0.62	0.80	0.74	0.31	0.81	46.3	0.59	136.51
17	1.15	16.20	0.90	0.71	0.69	0.69	0.88	0.51	0.42	0.67	45.7	0.71	126.20
18	1.19	14.35	1.45	0.71	0.72	0.72	0.84	0.74	0.46	0.86	44.2	0.60	125.11
19	1.19	14.35	0.90	0.71	0.66	0.86	0.89	0.70	0.32	0.70	45.5	0.79	130.37
20	1.15	14.35	1.18	0.71	0.66	0.76	0.92	0.92	0.42	0.62	45.1	0.82	132.35
21	1.15	12.50	1.45	0.71	0.71	0.82	0.87	0.66	0.45	0.74	44.8	0.65	128.10
22	1.10	14.35	1.18	0.46	0.67	0.77	0.85	0.77	0.32	0.70	43.3	0.76	122.92
23	1.10	16.20	1.18	0.71	0.69	0.89	0.82	0.72	0.43	0.87	43.5	0.56	126.45
24	1.15	14.35	1.45	0.96	0.75	0.75	0.88	0.70	0.42	0.59	44.2	0.68	132.63
25	1.15	14.35	1.18	0.71	0.78	0.78	0.88	0.88	0.41	0.62	43.8	0.78	123.15
26	1.19	16.20	1.18	0.71	0.59	0.79	0.86	0.86	0.41	0.89	43.2	0.76	123.33
27	1.19	14.35	1.18	0.46	0.59	0.59	0.88	0.53	0.55	0.55	44.6	0.68	132.43
28	1.10	14.35	1.45	0.71	0.54	0.74	0.84	0.74	0.31	0.73	45.4	0.76	126.76
29	1.10	14.35	1.18	0.96	0.57	0.57	0.87	0.63	0.42	0.82	43.9	0.52	121.18
Correlation degree					0.66		0.83		0.48		0.66		—
Proportion (%)					0.25		0.32		0.18		0.25		—

Note: *Mv* = measured value, *Cc* = correlation coefficient.

performance index, the evaluation index (Comprehensive Evaluation Index, CEI) for evaluating the high temperature performance of asphalt mixture is put forward, and the evaluation model of high temperature performance of aggregate is established based on the four morphological indexes of aggregate angularity  $X_1$ , needle flake content  $X_2$ , axial coefficient  $X_3$ , and convexity  $X_4$ . By embedding the evaluation model into the self-developed fast scanning and recognition system of coarse aggregate, it is more convenient to optimize or evaluate the aggregate at the construction site. The response surface test data are

shown in **Table 5**. Based on the Minitab platform, the step-by-step selection method is used to test the significance of the test data in **Table 6**, and the insignificant items are excluded (Yusoff et al., 2015).

The quadratic function of aggregate performance evaluation index, CEI, on  $X_1$ ,  $X_2$ ,  $X_3$ , and  $X_4$  is established by using Design Expert 8.0 software. The standard deviation of the fitting equation is summarized in **Table 7**.

Finally, the high temperature performance evaluation model of aggregate is shown in (6). The higher the CEI value, the better the high temperature performance of the aggregate.



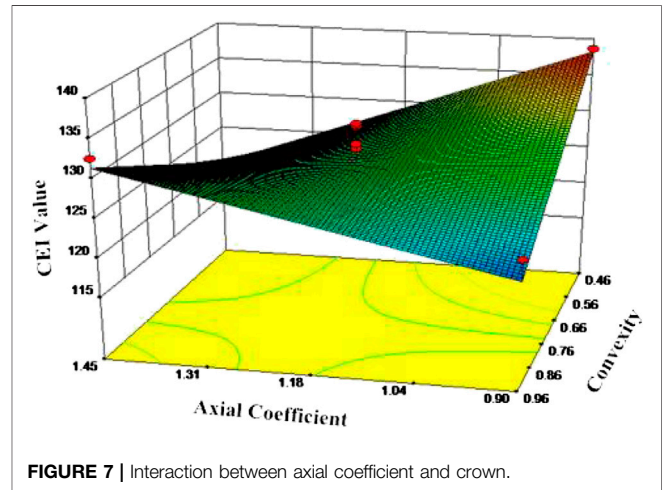
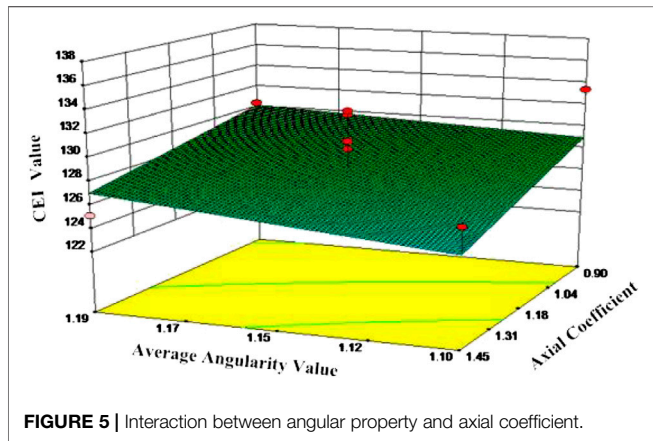
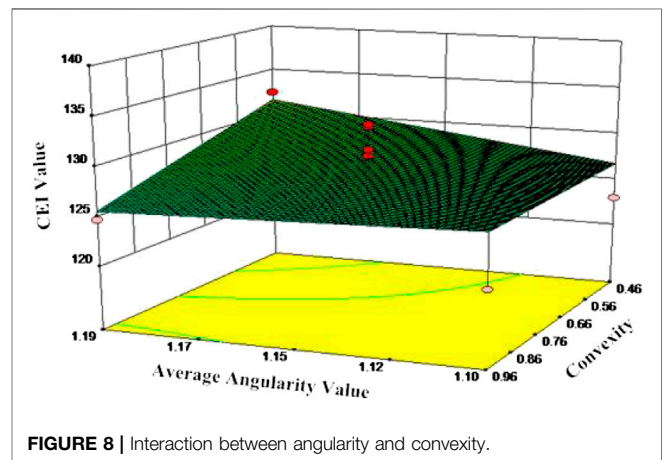
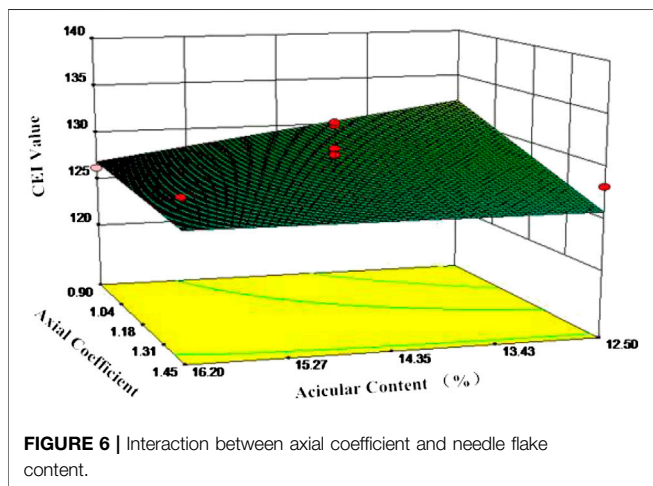


**TABLE 7 |** Summary of standard deviation of fitting equation.

S	R <sup>2</sup> (%)	R <sup>2</sup> (correction) (%)	R <sup>2</sup> (forecast) (%)
3,288	96.4	92.5	94.5



$$CEI = -255.59 + 471.69X_1 + 27.06X_2 - 151.87X_3 + 21.53X_4 - 27.09X_1X_2 + 27.27X_1X_3 - 132.89X_1X_4 + 2.72X_2X_3 + 0.07X_2X_4 + 105.20X_3X_4 \quad (6)$$

### Interaction Analysis of Morphological Indexes of Coarse Aggregate

In order to directly investigate the influence of the interaction of various factors on the high temperature performance of asphalt mixture, based on the above experimental data, the three-dimensional response surfaces of  $X_1$ ,  $X_2$ ,  $X_3$ , and  $X_4$  are established, as shown in **Figures 5–8**.

It can be seen from **Figure 5** that the larger the axial coefficient is, the smaller the CEI index is. This is because the larger the axial coefficient is, the flatter the aggregate is, which is more disadvantageous to the high temperature performance of

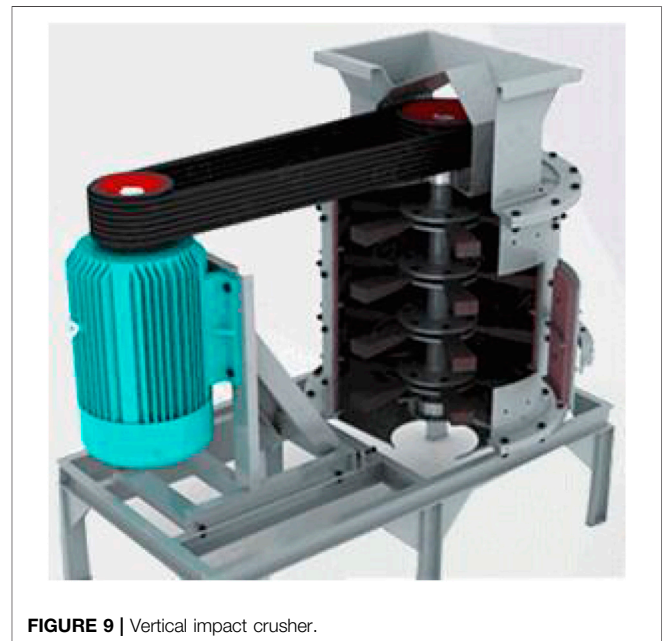


**TABLE 8** | Parameter combination of aggregate processing equipment.

ID	Factors			CEI
	Rotational speed (m/s)	Feed quantity (t/h)	Air volume (%)	
1	35	2	10	125.53
2	35	3	20	131.47
3	35	4	30	128.63
4	45	3	30	141.75
5	45	4	10	130.24
6	45	2	20	122.46
7	55	4	20	125.37
8	55	2	30	130.49
9	55	3	10	134.71

asphalt mixture. With the increase of the angular value, the CEI index value becomes larger, indicating that the angular value is positively correlated with the high temperature performance (Hülsheger et al., 2011). As can be seen from **Figure 6**, there is a negative correlation between axial coefficient, needle-like content, and CEI evaluation index, which is consistent with the actual situation. As can be seen from **Figure 7**, the smaller the convexity is, the smaller the actual area of the aggregate and the area of the circumscribed polygon are and the rougher the aggregate surface is, which is beneficial to the high temperature performance. On the other hand, the smaller the axial coefficient is, the closer the aggregate particles are to spherical or square, which will improve the high temperature performance of asphalt mixture. When the convexity and axial coefficient are taken to the minimum, the CEI evaluation index reaches the maximum value. It can be seen from **Figure 8** that the smaller the convexity is, the smaller the actual area of aggregate and the area of circumscribed polygon are and the better the angularity is. Therefore, when the convexity takes the minimum value and the angularity takes the maximum value, the evaluation index CEI of high temperature performance of asphalt mixture reaches the maximum value.

## Optimization and Verification of Processing Parameters of Coarse Aggregate

The proposed aggregate performance evaluation index CEI is embedded into the aggregate shape recognition system CAMIS, and the parameters of the vertical shaft impact aggregate crusher are optimized based on the improved CAMIS system, as shown in **Figure 9**.

Select the combination of three factors and three levels of parameters, including rotational speed (35, 45, 55 m/s), feed quantity (2, 3, 4 t/h), and air intake (10, 20, 30%). The experiment was designed based on the L9 (3<sup>4</sup>) orthogonal table, as shown in **Table 8**.

As can be seen from **Table 7**, the CEI value of the fourth group of processing parameters is the largest, so the processing parameters of S3 jaw crusher are recommended as rotational speed: 45 m/s feed: 3 t/h air intake: 30%. The recommended processing parameters are verified by laboratory tests, and the dynamic stability, dynamic modulus, maximum shear stress, and internal friction angle are selected as verification indexes, respectively. The aggregates needed for the test are prepared by using the processing parameters in **Table 7**, and the preparation parameters and test methods of the asphalt mixture used are the same as the previous ones, and the test results are shown in **Table 9**.

It can be seen from **Table 8** that the high temperature performance index corresponding to the fourth group of aggregate processing parameters is the best, and the results are consistent with the above, so the aggregate evaluation index CEI proposed in this article can be used to evaluate the high temperature performance of regional aggregates.

## CONCLUSIONS

- (1) A simple and economical coarse aggregate morphological feature recognition system (CAMIS) is developed based on computer vision technology. The system can identify needle-like content, axial coefficient, angular value, and convexity of aggregates above 2.36 mm particle size, can supply materials uninterruptedly, and realize mass inspection. The response time of single aggregate is less than 1 s.
- (2) Based on the CAMIS system, combined with the laboratory test, it is concluded that the impact factor of the morphological characteristics of coarse aggregate on the high temperature performance is angular > needle flake > axial coefficient > crown.
- (3) The evaluation model of high temperature performance of aggregate is established by using the improved response surface design method, the aggregate evaluation index CEI is put forward, and the effect of pairwise interaction of each morphological index on CEI index is analyzed. The results

**TABLE 9** | Verification of the test results.

Processing parameters	Dynamic stability (KN)	Dynamic modulus (Gpa)	Maximum shear stress (Mpa)	Internal friction angle (°)
1 (35, 2, 10)	12.6	1.48	0.82	45.3
2 (35, 3, 20)	12.9	1.43	0.85	44.2
3 (35, 4, 30)	11.7	1.52	0.78	45.2
4 (45, 3, 30)	14.9	1.57	0.94	46.9
5 (45, 4, 10)	13.9	1.39	0.88	44.7
6 (45, 2, 20)	14.3	1.45	0.82	45.7
7 (55, 4, 20)	13.7	1.51	0.76	43.8
8 (55, 2, 30)	13.2	1.37	0.84	46.3
9 (55, 3, 10)	12.5	1.47	0.91	45.7

show that CEI index can be used to evaluate the high temperature performance of aggregate.

- (4) The proposed aggregate performance evaluation index CEI is integrated into the aggregate shape recognition system CAMIS, and the parameters of S3 jaw aggregate crusher are optimized. The combination of processing parameters is recommended as rotational speed: 45 m/s feed: 3 t/h air intake: 30%. Laboratory tests show that the aggregate identification system CAMIS and the aggregate performance evaluation index CEI developed in this study are of high reliability.

## DATA AVAILABILITY STATEMENT

The original contributions presented in the study are included in the article/Supplementary Material; further inquiries can be directed to the corresponding author.

## REFERENCES

- Al-Rousan, T., Masad, E., Tutumluer, E., and Pan, T. (2007). Evaluation of image analysis techniques for quantifying aggregate shape characteristics. *Construct. Build. Mater.* 21 (5), 978–990. doi:10.1016/j.conbuildmat.2006.03.005
- Arasan, S., Yenera, E., Hattatoglu, F., Hınıslioglu, S., and Akbuluta, S. (2011). Correlation between shape of aggregate and mechanical properties of asphalt concrete: digital image processing approach. *Road Mater. Pavement Des.* 12 (2), 239–262. doi:10.3166/rmpd.12.239-262
- Chen, M., Tang, Y., Zou, X., Huang, K., Li, L., and He, Y. (2019). High-accuracy multi-camera reconstruction enhanced by adaptive point cloud correction algorithm. *Optic Laser. Eng.* 122, 170–183. doi:10.1016/j.optlaseng.2019.06.011
- Ding, X., Ma, T., and Gao, W. (2017). Morphological characterization and mechanical analysis for coarse aggregate skeleton of asphalt mixture based on discrete-element modeling. *Construct. Build. Mater.* 154, 1048–1061. doi:10.1016/j.conbuildmat.2017.08.008
- Gao, J., Wang, H., Bu, Y., You, Z., Hasan, M. R. M., and Irfan, M. (2018). Effects of coarse aggregate angularity on the microstructure of asphalt mixture. *Construct. Build. Mater.* 183, 472–484. doi:10.1016/j.conbuildmat.2018.06.170
- Ghuzlan, K. A., Obaidat, M. T., and Alawneh, M. M. (2019). Cellular-phone-based computer vision system to extract shape properties of coarse aggregate for asphalt mixtures. *JESTECH.* 22 (3), 767–776. doi:10.1016/j.jestech.2019.02.003
- Hülshager, T., Brandt, C., Caon, A., Fiebrich, H. K., and Andreev, T. (2011). “The angular performance behavior of triple junction solar cells with different antireflection coatings for high temperature space missions,” in Proc. 9th European Space Power Conference, October, 2011, Saint Rafael, France: ESA Special Publication.
- JTG E42-2005 (2005). *Test methods of aggregate for highway engineering*. Beijing, China: China Ministry of Transport.
- JTG E20-2011, (2011). *Standard Test methods of Bitumen and Bituminous Mixture for Highway Engineering*. Beijing, China: China Ministry of Transport.
- Kuang, D., Wang, X., Jiao, Y., Zhang, B., Liu, Y., and Chen, H. (2019). Influence of angularity and roughness of coarse aggregates on asphalt mixture performance. *Construct. Build. Mater.* 200, 681–686. doi:10.1016/j.conbuildmat.2018.12.176
- Kwon, J., Kim, S. H., Tutumluer, E., and Wayne, M. H. (2017). Characterization of unbound aggregate materials considering physical and morphological properties. *Int. J. Pavement Eng.* 18 (4), 303–308. doi:10.1080/10298436.2015.1065997
- Lei, Z., Bahia, H., and Yi-qiu, T. (2015). Effect of bio-based and refined waste oil modifiers on low temperature performance of asphalt binders. *Construct. Build. Mater.* 86, 95–100. doi:10.1016/j.conbuildmat.2015.03.106
- Li, B., Zhang, C., Xiao, P., and Wu, Z. (2019). Evaluation of coarse aggregate morphological characteristics affecting performance of heavy-duty asphalt pavements. *Construct. Build. Mater.* 225, 170–181. doi:10.1016/j.conbuildmat.2019.07.092
- Liu, Y., Sun, W., Nair, H., Stephen Lane, D., and Wang, L. (2016). Quantification of aggregate morphologic characteristics as related to mechanical properties of asphalt concrete with improved FTI system. *J. Mater. Civ. Eng.* 28 (8), 04016046. doi:10.1061/(asce)mt.1943-5533.0001535
- Liu, Z., Cao, Y., Wang, Y., and Wang, W. (2019). Computer vision-based concrete crack detection using U-net fully convolutional networks. *Autom. Construct.* 104, 129–139. doi:10.1016/j.autcon.2019.04.005
- Luo, X., Wang, Y., Zhao, J., Chen, Y., Mo, S., and Gong, Y. (2016). Grey relational analysis of an integrated cascade utilization system of geothermal water. *Int. J. Green Energy* 13 (1), 14–27. doi:10.1080/15435075.2014.896259
- Majidifard, H., Adu-Gyamfi, Y., and Buttler, W. G. (2020). Deep machine learning approach to develop a new asphalt pavement condition index. *Construct. Build. Mater.* 247, 118513. doi:10.1016/j.conbuildmat.2020.118513
- Mohamed, O. A., Masood, S. H., and Bhowmik, J. L. (2016). Mathematical modeling and FDM process parameters optimization using response surface methodology based on Q-optimal design. *Appl. Math. Model.* 40 (23–24), 10052–10073. doi:10.1016/j.apm.2016.06.055
- Mourabet, M., El Rhilassi, A., El Boujaady, H., Bennani-Ziatni, M., El Hamri, R., and Taitai, A. (2012). Removal of fluoride from aqueous solution by adsorption on Apatitic tricalcium phosphate using Box–Behnken design and desirability function. *Appl. Surf. Sci.* 258 (10), 4402–4410. doi:10.1016/j.apsusc.2011.12.125
- Plati, C., Georgiou, P., and Loizos, A. (2016). Influence of different roller compaction modes on asphalt mix performance. *Int. J. Pavement Eng.* 17 (1), 64–70. doi:10.1080/10298436.2014.925552
- Rezaei, A., and Masad, E. (2013). Experimental-based model for predicting the skid resistance of asphalt pavements. *Int. J. Pavement Eng.* 14 (1), 24–35. doi:10.1080/10298436.2011.643793
- Shen, C., Shen, B., Xu, H., Bai, J., Dai, L., Lv, Q., et al. (2014). Formulation and optimization of a novel oral fast dissolving film containing drug nanoparticles by Box–Behnken design–response surface methodology. *Drug Dev. Ind. Pharm.* 40 (5), 649–656. doi:10.3109/03639045.2014.884116
- Singh, D., Zaman, M., and Commuri, S. (2013). “Comparison of morphological properties of different types of coarse aggregates,” in *Airfield and Highway pavement 2013: sustainable and efficient pavements*, 1254–1263.
- Tang, Y., Li, L., Wang, C., Chen, M., Feng, W., Zou, X., et al. (2019). Real-time detection of surface deformation and strain in recycled aggregate concrete-filled steel tubular columns via four-ocular vision. *Robot. Comput. Integrated Manuf.* 59, 36–46. doi:10.1016/j.rcim.2019.03.001
- Tasdemir, Y. (2009). High temperature properties of wax modified binders and asphalt mixtures. *Construct. Build. Mater.* 23 (10), 3220–3224. doi:10.1016/j.conbuildmat.2009.06.010
- Wang, H., Bu, Y., Wang, Y., Yang, X., and You, Z. (2016). The effect of morphological characteristic of coarse aggregates measured with fractal

## AUTHOR CONTRIBUTIONS

ZL designed the experiments and wrote the paper; LS performed the experiments; JW analyzed the data; CZ contributed materials and funding. We confirm that the order of authors listed in the manuscript has been approved by all named authors. All authors have read and agreed to the published version of the manuscript.

## FUNDING

This research was funded by the China Postdoctoral Science Foundation (2020M683402), Open Fund of Key Laboratory for Special Area Highway Engineering of Ministry of Education (Chang’an University) (Program no. 300102210504), and the Science and Technology Planning Project of Xi’an (Program no. 2020KJRC0046).

- dimension on asphalt mixture's high-temperature performance. *Adv. Mater. Sci.* 2016, 1–9. doi:10.1155/2016/6264317
- Wang, A., Zhang, Z., Liu, K., Xu, H., Shi, L., and Sun, D. (2019a). Coral aggregate concrete: numerical description of physical, chemical and morphological properties of coral aggregate. *Cement Concr. Compos.* 100, 25–34. doi:10.1016/j.cemconcomp.2019.03.016
- Wang, Z., Li, H., and Zhang, X. (2019b). Construction waste recycling robot for nails and screws: computer vision technology and neural network approach. *Autom. ConStruct.* 97, 220–228. doi:10.1016/j.autcon.2018.11.009
- Yusoff, N., Saad, N. H., Nabipoor, M., Sulaiman, S., Ghawi, N. M. M. A., Jaffar, A., et al. (2015). Design of experiment using Minitab for screening breath sensor workability performance. *Jurnal Teknologi.* 76 (9), 1–5. doi:10.11113/jt.v76.5635
- Zhang, D., Huang, X., and Zhao, Y. (2012). Investigation of the shape, size, angularity and surface texture properties of coarse aggregates. *Construct. Build. Mater.* 34, 330–336. doi:10.1016/j.conbuildmat.2012.02.096

**Conflict of Interest:** The authors declare that the research was conducted in the absence of any commercial or financial relationships that could be construed as a potential conflict of interest.

Copyright © 2021 Liu, Zhang, Shao and Wang. This is an open-access article distributed under the terms of the Creative Commons Attribution License (CC BY). The use, distribution or reproduction in other forums is permitted, provided the original author(s) and the copyright owner(s) are credited and that the original publication in this journal is cited, in accordance with accepted academic practice. No use, distribution or reproduction is permitted which does not comply with these terms.